Palmprint Identification Using LBP and Different Representations

Yang Zhao[1,2], Wei Jia[1], RongXiang Hu[1,2] and Jie Gui[1]

[1] Intelligent Computing Laboratory, Hefei Institute of Intelligent Machines, Chinese Academy of Sciences, P.O.Box 1130, Hefei, 230031, China

[2] Department of Automation, University of Science and Technology of China, Hefei 230027, China

zyknight@mail.ustc.edu.cn

Abstract— **In this paper, a new Local Binary Pattern (LBP) and Local Ternary Pattern (LBP) based palmprint identification method is proposed. In our method, LBP or LTP descriptor is applied to the energy or direction representations of palmprint extracted by the modified finite radon transformation (MFRAT). Experimental results obtained from the Hong Kong Polytechnic University (PolyU) Palmprint Database demonstrate that the proposed method has higher identification rates than other LBP based methods.**

Keywords-palmprint identification, local binary pattern, local ternary pattern, MFRAT

I. INTRODUCTION

In recent years, hand based biometric [1][20~26], especially palmprint recognition has drawn wide attention from researchers. Compared with other biometric technologies, palmprint based biometric has several advantages such as stable line features, low-resolution imaging, less image distortion and easy self positioning. Besides, it can obtain high accurate recognition rate with fast processing speed [1].

Generally, the approaches for palmprint recognition can be roughly divided into several different categories. A. Kong *et al*. has made a survey on these approaches [2]. Texture based approaches usually exploit Fourier Transform, Wavelet Transform (WT), Ridgelet Transform, Contourlet Transform and Local Binary Pattern (LBP) to extract texture features for recognition. Line based approaches often focus on extracting principal lines-like and crease features for recognition [3-5]. Subspace learning approaches have also been used for palmprint recognition, but they are sensitive to illumination, slight translation and rotation changes. Orientation based approaches have good performance since they are robust to different illumination conditions [6, 7].

Local Binary Pattern (LBP) proposed by T. Ojala *et al*. [8] is a powerful local image descriptor, which has been successfully adopted for many applications such as face recognition [9], texture classification, object and scene recognition. Recently, the research on LBP has made a great progress. For example, some variants of LBP have been proposed including Local Ternary Pattern (LTP) [10], dominant LBP (DLBP) [11], center-symmetric LBP (CS-LBP) [12], Local Derivative Pattern (LDP) [13], and completed LBP (CLBP) [14], etc. As we have mentioned above, LBP plays an important role in face recognition field. Ahone *et al*. [9] proposed to use LBP in face recognition based on the fact that faces can be seen as a composition of micro-patterns which can be well described by local operator. Analogously, LBP has also been applied to palmprint recognition [18]. LBP, however, still has some shortcomings, *e.g*, it is sensitive to noise and can not effectively extract features related to scale, orientation and localization. Since Gabor wavelet is a powerful tool to extract spatial structure of an object, some researcher proposed some methods combining Gabor wavelet representation and LBP. W. Zhang *et al*. [15] proposed a new LBP descriptor in Gabor transform domain (LGBP). Then, B .Zhang *et al*. [16] proposed to combine Gabor phase information with LBP (LGPP). Later, S.F. Xie *et al*. [17] proposed local XOR pattern integrating with Gabor transform (LGXP).

Although these Gabor based local operators have achieved well performance, they have to face a serious problem, i.e., using Gabor wavelet to extract multi-scale and multi-orientation features has high computational-complexity. In this paper, we propose a new LBP based palmprint recogniton method, in which the modified finite radon transformation (MFRAT) is exploited to extract the line energy and direction maps of a palmprint image. Compared with Gabor wavelet, MFRAT has fast speed for feature extraction. On the other hand, LTP extends LBP to 3-valued codes by adding a user-specified threshold, therefore, it is more discriminative. In this paper, we apply LBP and LTP descriptors to the energy and direction representations of palmprint extracted by MFRAT. Meanwhile, the Chi-square distance and the nearest neighbor rule (1NN) are exploited for classification.

The main contributions of this paper are presented as follows: (1) It is the first time that the LBP and LTP descriptors are applied to the direction representation of palmprint; (2) We prove that combining LTP and direction representation can obtain better identification rate; (3) For palmprint identification, the performance of the proposed method is better than other LBP based methods.

The rest of this paper is organized as follows: Section II briefly reviews LBP and LTP descriptors. Section III presents how to extract energy and direction representations of palmprint by MFRAT. Section IV reports experimental results. Section V concludes the whole paper.

978-1-4577-0490-1/11/$26.00 ©2011 IEEE

II. Brief Review of LBP and LTP Descriptors

A. Local Binary Pattern

In literature [8], T. Ojala et al. proposed LBP descriptor to characterize the spatial structure of the local image texture. LBP code is computed by comparing a pixel with its neighbors, which can be described by the following formula:

$$LBP_{P,R}=\sum_{p=0}^{P-1}s(g_p-g_c)2^p,\qquad s(x)=\begin{cases}1, x\ge 0\\ 0, x<0\end{cases} \tag{1}$$

where g_c represents the gray value of the center pixel and $g_p(p=0,\cdots,P\text{-}1)$ denotes the gray value of its neighbor on a circle of radius R, and P is the total number of the neighbors. It should be noted that the neighbors that do not fall in the center of pixels can be estimated by bilinear interpolation.

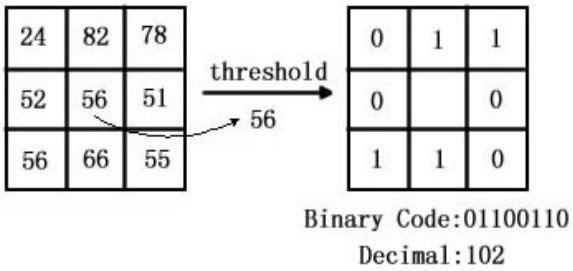

Fig.1. Illustration of LBP (P=8, R=1)

LBP encoding process is illustrated in Fig. 1. The values of eight neighbors are turned into 0 or 1 by using the central value 56 as the threshold. Then the decimal code 102 is set as the LBP code of the central pixel. After the LBP code of each pixel is defined, a histogram is built to represent the texture feature.

B. Local Ternary Pattern

LBP is sensitive to noise since only using the value of center pixel as a threshold can not robustly reflect the texture changes in near-uniform image regions. X. Tan *et al*. [10] extended LBP to 3-valued LTP. The construction of LTP descriptor can be described by the following formula:

$$LTP_{P,R}=\sum_{p=0}^{P-1}s(g_p-g_c)2^p,\qquad s(x)=\begin{cases}1, x\ge t\\ 0, |x|<t\\ -1, x<-t\end{cases} \tag{2}$$

where t is a threshold specified by user. As being illustrated in Fig. 2, conventional 2-valued (0, 1) LBP code is extended to 3-valued (-1, 0, 1) ternary code by using threshold t. Then the upper pattern and lower pattern are coded, respectively. LTP codes are more robust to noise, but no longer strictly invariant to monotonic gray scale transformation.

III. Extracting Energy and Direction Representations Using MFRAT

MFRAT was initially proposed to extract principal lines [5]. Experimental results reported in [5][7] have shown that MFRAT is a powerful tool to effectively extract palm line's energy and orientation features. Additionally, another advantage of the MFRAT is its computational efficiency. It runs very fast since only addition operation is involved. On the contrary, the convolution between one image and Gabor wavelet involves a mass of multiplication operations.

In this paper, we use MFRAT to extract energy and direction representations of palmprints. Here, the MFRAT is defined as follows:

Denoting $Z_p=\{0,1,\ldots,p\text{-}1\}$, where p is a positive integer, the MFRAT of real function $f[x,y]$ on the finite grid Z_p^2 is defined as:

$$r[L_k]=MFRAT_f(k)=\sum_{i,j\in L_k}f[i,j] \tag{3}$$

where L_k denotes the set of points that make up a line on the lattice Z_p^2, which means:

$$L_k=\{(i,j): j=S_k(i-i_0)+j_0, i\in Z_p\} \tag{4}$$

where (i_0,j_0) denotes the center point of the lattice Z_p^2, and k means the index value corresponding to the slope of S_k. That is to say, different k denotes different slopes of L_k. For any given k, the summation of only one line, which passes through the

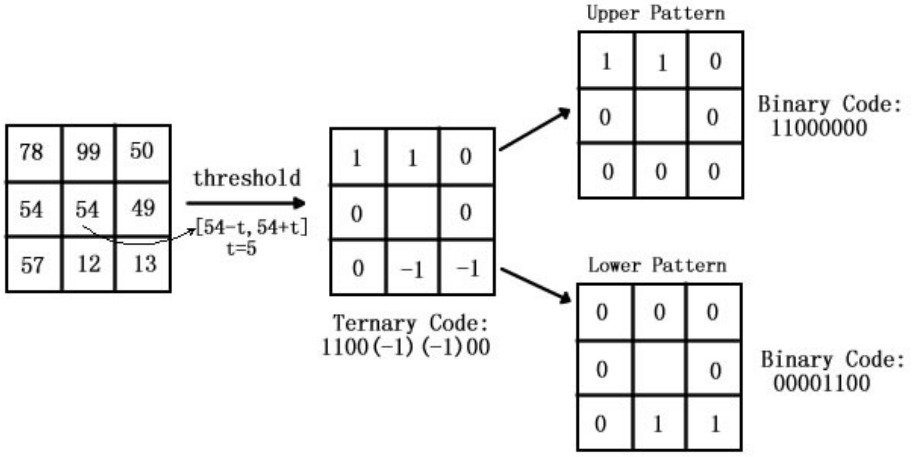

Fig. 2. Illustration of LTP (P=8, R=1).

center point (i_0,j_0) of Z_p^2, is calculated. It should be pointed out that all lines at different directions have an identical number of pixels.

And note that before taking the MFRAT given in Eqn. (3), the mean should be subtracted from an input *f'*, thus we have:

$$f = f' - mean(f') \tag{5}$$

$$\sum f[i,j] = 0 \qquad (i,j) \in Z^2{}_p \tag{6}$$

In MFRAT, the direction θ_k and the energy *e* of center point $f(i_0, j_0)$ of the lattice Z^2_p are calculated by following formula :

$$\theta_{k(i_0,j_0)} = \arg(\min_k(r[L_k])) \quad k = 1,2,\cdots N \tag{7}$$

$$e_{(i_0,j_0)} = \left|\min(r[L_k])\right| \quad k = 1,2,\cdots N \tag{8}$$

where $|\cdot|$ denotes the absolute operation.

In this way, the directions and energies of all pixels are calculated if the center of lattice Z^2_p moves over an image pixel by pixel. For an image *I(x,y)* of size *m*×*n*, if the values of all pixels are replaced by their energies and index values of directions, two new images, i.e., Energy_image and Direction_image can be created, respectively.

$$Energy\_image = \begin{vmatrix} e_{(1,1)} & e_{(1,2)} & \vdots & e_{(1,n)} \\ e_{(2,1)} & e_{(2,2)} & \vdots & e_{(2,n)} \\ \cdots & \cdots & \cdots & \cdots \\ e_{(m,1)} & e_{(m,2)} & \vdots & e_{(m,n)} \end{vmatrix}$$

$$Direction\_image = \begin{vmatrix} k(1,1) & k(1,2) & \vdots & k(1,n) \\ k(2,1) & k(2,2) & \vdots & k(2,n) \\ \cdots & \cdots & \cdots & \cdots \\ k(m,1) & k(m,2) & \vdots & k(m,n) \end{vmatrix}$$

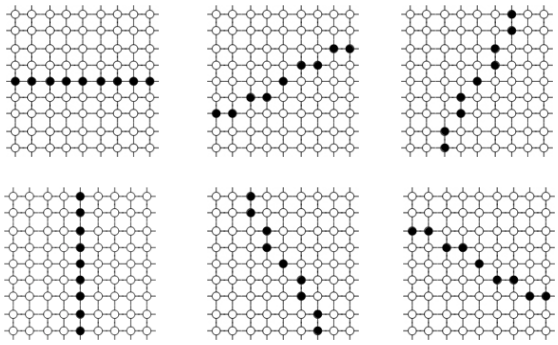

Fig. 3. 9×9 MFRAT at six directions

Fig. 3 shows an example of the 9×9 MFRAT whose lines, $L(\theta_k)$, are at directions of 0°, $\pi/6$, …, and $5\pi/6$, respectively. If the line in the MFRAT is 1 pixel wide, *p* should be an odd number in order to clearly define the center of Z^2_p. Here, it should be noted that in order to view the directional representation clearly, we multiply the value of directions by 20 to construct the final direction image. Fig. 4 illustrates an example of extracting energy and direction representations using MFRAT.

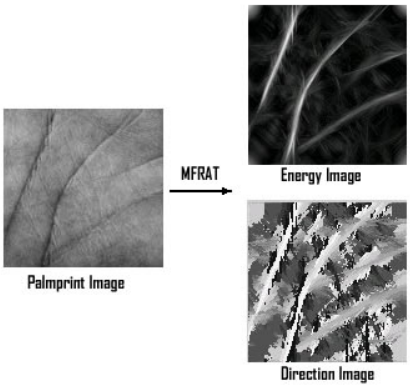

Fig. 4. An example of extracting energy and direction representations using MFRAT

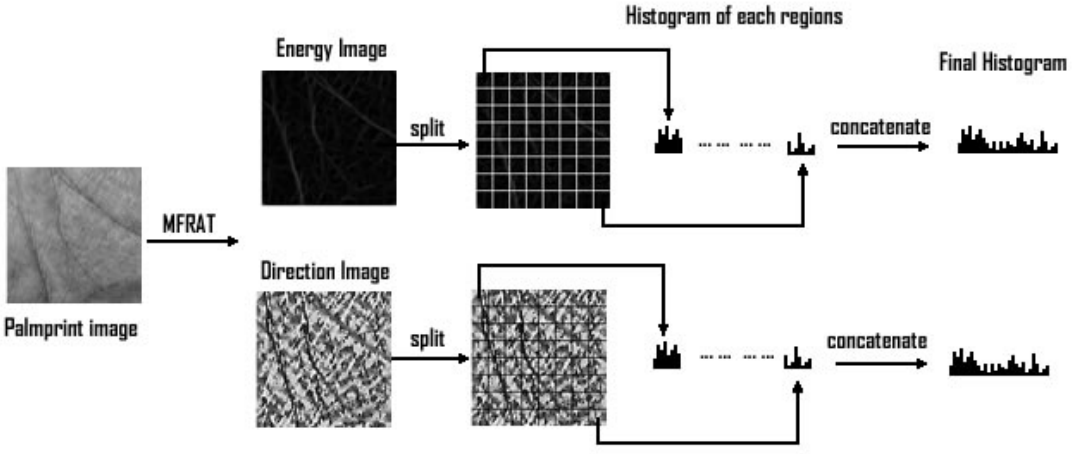

Fig. 5. The framework of the proposed method

TABLE I. ACCURACY (%) OF DIFFERENT MFRAT SIZES.

Method	size11	size13	size15	size17	size19	size21	size23	size25	size27	size29	size31	size33
Direction Image +LBP	94.12	95.91	96.82	97.23	98.89	99.07	99.22	99.56	99.33	99.33	99.46	99.46
Energy Image +LBP	96.87	97.28	97.67	97.67	98.86	99.28	99.04	99.02	99.25	99.07	99.07	99.24
Direction Image +LTP	98.11	98.84	99.17	99.53	99.28	99.72	99.69	99.79	99.82	99.79	99.50	99.12

TABLE II. COMPARISONS BETWEEN LOCAL GABOR BASED METHODS AND THE PROPOSED METHODS

Method	Accuracy (%)	Final Feature Length	Histogram length
LBP + Original Image	82.32	59	3776
LGBP_Mag [18]	95.86	10240	40960
LGBP_Phase [18]	97.67	10240	40960
HGPP [18]	98.40	10240	92160
LGXP [18]	98.24	10240	40960
LTP + Direction Image (The proposed method)	**99.82**	118	7552

IV. THE PROPOSED METHOD

A. The framework of the proposed method

As we have mentioned above, directly applying LBP descriptor to original palmprint image can not obtain promising recognition performance. Using Gabor based representation can help LBP descriptor improve recognition performance, but calculating Gabor based representation has high computational-complexity. In our approach, we use MFRAT to extract the energy and direction representations of palmprint, and apply LBP or LTP descriptors to these representations for recognition.

Fig. 5 illustrates the framework of the proposed method. First, palmprint image is transformed to energy image and directional image by applying MFRAT. Second, each energy or direction image is divided into non-overlapping regions, and LBP or LTP histogram is computed for each region. Lastly, the histograms of regions are concatenated to form the final histogram. Here, it should be noted that LTP is only applied to direction representation since direction representation is more robust to illumination changes than energy representation.

B. Similarity measurement for histogram

Chi-square distance (χ^2) is exploited as similarity measurement which is calculated as follows:

$$d_{\chi^2} = \sum_{b=0}^{B-1} \frac{(H_f^b - H_I^b)^2}{(H_f^b + H_I^b)} \quad (9)$$

where $d\chi^2$ denotes similarity of image f and I, H_f and H_I with B bins denote the histogram of image f and I. Then the classifier of 1NN is used for classification.

V. EXPERIMENTS

A. Database

The proposed method was tested on the Hong Kong Polytechnic University (PolyU) Palmprint Database II. This database contains 7752 grayscale palmprint images from 386 palms corresponding to 193 individuals. In this database, about 20 samples from each of these palms were collected in two sessions, where about 10 samples were captured in the first session and the second session, respectively. The total numbers of images captured in the first session and the second session are 3889 and 3863, respectively. The average interval between the first and the second collection is two months. The resolution of all the original palmprint images is 384×284 pixels at 75 dpi. A detailed introduction of Database II can be found in [1]. In our paper, by using the similar preprocessing approach described in literature [1], palmprint is orientated and the ROI, whose size is 128×128, is cropped.

In our experiments, we use first three palmprints from the first session for training and leave the palmprints from the second session for test. Therefore, the numbers of images for training and test are 1158 and 3863, respectively.

B. Experimental results

In the first experiment, we use MFRATs with different sizes to generate the energy images and direction images. LTP is merely applied on direction images (LTP + Direction Image) and LBP is applied on both energy images (LBP + Energy Image) and direction images (LBP + Direction Image). In our experiment, each energy or direction image is divided into 8×8 non-overlapping regions, and LBP uniform feature (59 bins) or LTP uniform feature (118 bins) is computed for each region. Thus the total histogram length of LBP + Energy Image or LBP + Direction Image is 3776 (8×8×59) and the total length of LTP + Direction Image is 7552 (8×8×118). The identification results are listed in Table I. From this table, it

can be seen that the proposed method achieves good identification rates when the size of MFRAT is in the range of {21, 23, 25, 27}, and the method of LTP + Direction Image achieves the highest identification rate, which is 99.82%.

We also make a performance comparison between the proposed method and other methods, which is shown in Table II. We firstly test the performance of LBP on original palmprint images (LBP + Original Image). We also divide original image into 8x8 regions, and then extract LBP uniform feature (59 bins) in each region. It can be seen that the identification rate of LBP + Original Image is 82.32%, which is much lower than that of the proposed method. In order to compare with local Gabor based operators such as LGBP_Magnitude [15], LGBP_Phase [19], HGPP [16], and LGXP [17], we cite their identification rates reported in literature [18]. For each Gabor based method listed in Table II, 5-scale and 8-orientation Gabor filter bank is used for feature extraction. Each local Gabor pattern matrix is partitioned into 2×2 subblocks. In each subblock, LBP or LXP histogram is computed. Table II also clearly shows that the performance of the proposed method is better than that of those local Gabor based methods, meanwhile, the feature length of the proposed method is much shorter. It should be noted that five samples from each class in session one are chosen to construct the training set in these local Gabor based method [18], but in our approaches, only three samples in session one are used for training.

VI. CONCLUSION

This paper is motivated by the fact that current LBP based palmprint recognition methods have various demerits. We proposed to use MFRAT to reduce the noise interference so that LBP can get better results. Besides, the direction image of MFRAT is invariant to the illumination changes so that the LTP descriptor can be ideally applied to these direction images. The experimental results have shown that the proposed method can get higher identification rates than other LBP based methods.

ACKNOWLEDGMENT

This work is supported by the grants of the National Science Foundation of China, No. 61175022, 61100161, 61005010, 60705007, 60975005 and 60805021; and the grants of the Knowledge Innovation Program of the Chinese Academy of Sciences (Y023A11292 & Y023A61121).

REFERENCES

[1] D. Zhang, W. K. Kong, J. You et al., “Online palmprint identification,” IEEE Transactions on Pattern Analysis and Machine Intelligence, vol. 25, no. 9, pp. 1041-1050, Sep, 2003.

[2] A. Kong, D. Zhang, and M. Kamel, “A survey of palmprint recognition,” Pattern Recognition, vol. 42, no. 7, pp. 1408-1418, Jul, 2009.

[3] L. Zhang, and D. Zhang, “Characterization of palmprints by wavelet signatures via directional context modeling,” IEEE Transactions on Systems Man and Cybernetics Part B-Cybernetics, vol. 34, no. 3, pp. 1335-1347, Jun, 2004.

[4] X. Q. Wu, D. Zhang, K. Q. Wang et al., “Palmprint classification using principal lines,” Pattern Recognition, vol. 37, no. 10, pp. 1987-1998, Oct, 2004.

[5] D. S. Huang, W. Jia, and D. Zhang, “Palmprint verification based on principal lines,” Pattern Recognition, vol. 41, no. 4, pp. 1316-1328, Apr, 2008.

[6] A. W. K. Kong, and D. Zhang, “Competitive coding scheme for palmprint verification,” Proceedings of the 17th International Conference on Pattern Recognition, Vol 1, pp. 520-523, 2004.

[7] W. Jia, D. Huang, and D. Zhang, “Palmprint verification based on robust line orientation code,” Pattern Recognition, vol. 41, no. 5, pp. 1504-1513, May, 2008.

[8] T. Ojala, M. Pietikainen, and T. Maenpaa, “Multiresolution gray-scale and rotation invariant texture classification with local binary patterns,” IEEE Transactions on Pattern Analysis and Machine Intelligence, vol. 24, no. 7, pp. 971-987, Jul, 2002.

[9] T. Ahonen, A. Hadid, and M. Pietikainen, “Face description with local binary patterns: Application to face recognition,” IEEE Transactions on Pattern Analysis and Machine Intelligence, vol. 28, no. 12, pp. 2037-2041, Dec, 2006.

[10] X. Y. Tan, and B. Triggs, “Enhanced Local Texture Feature Sets for Face Recognition Under Difficult Lighting Conditions,” IEEE Transactions on Image Processing, vol. 19, no. 6, pp. 1635-1650, Jun, 2010.

[11] S. Liao, M. W. K. Law, and A. C. S. Chung, “Dominant Local Binary Patterns for Texture Classification,” IEEE Transactions on Image Processing, vol. 18, no. 5, pp. 1107-1118, May, 2009.

[12] M. Heikkila, M. Pietikainen, and C. Schmid, “Description of interest regions with local binary patterns,” Pattern Recognition, vol. 42, no. 3, pp. 425-436, Mar, 2009.

[13] B. C. Zhang, Y. S. Gao, S. Q. Zhao et al., “Local Derivative Pattern Versus Local Binary Pattern: Face Recognition With High-Order Local Pattern Descriptor,” IEEE Transactions on Image Processing, vol. 19, no. 2, pp. 533-544, Feb, 2010.

[14] Z. H. Guo, L. Zhang, and D. Zhang, “A Completed Modeling of Local Binary Pattern Operator for Texture Classification,” IEEE Transactions on Image Processing, vol. 19, no. 6, pp. 1657-1663, Jun, 2010.

[15] W. C. Zhang, S. G. Shan, W. Gao et al., “Local gabor binary pattern histogram sequence (LGBPHS): A novel non-statistical model for face representation and recognition,” Tenth Ieee International Conference on Computer Vision, Vols 1 and 2, Proceedings, pp. 786-791, 2005.

[16] B. H. Zhang, S. G. Shan, X. L. Chen et al., “Histogram of Gabor phase patterns (HGPP): A novel object representation approach for face recognition,” IEEE Transactions on Image Processing, vol. 16, no. 1, pp. 57-68, Jan, 2007.

[17] S. F. Xie, S. G. Shan, X. L. Chen et al., “Fusing Local Patterns of Gabor Magnitude and Phase for Face Recognition,” IEEE Transactions on Image Processing, vol. 19, no. 5, pp. 1349-1361, May, 2010.

[18] M. Mu, Q. Ruan, and S. Guo, “Shift and gray scale invariant features for palmprint identification using complex directional wavelet and local bianry pattern,” Neurocomputing, to appear.

[19] W. Zhang, S. Shan, et al., "Are Gabor phase really useless for face recognitionb?," in Proc. IEEE Int. Conf. Pattern Recogn, 606-609, 2006

[20] D. Zhang, Z.H. Guo, et al., "An online system of multispectral palmprint verification," IEEE Trans. on Instrument and Measurement, voll.59, no. 2, pp. 480-490, 2010.

[21] D. Zhang, Z.H. Guo, G.M. Lu, L. Zhang, et al., "Online joint palmprint and palmvein verification," Expert System with Applications, vol. 38, no. 3, pp. 2621-2631, 2011

[22] Z.H. Guo, W.M. Zuo, L. Zhang, D. Zhang,"A unified distance measurement for orientation coding in palmprint verification," Neurocomputing, vol. 73, pp. 944-950, 2010

[23] L. Zhang, L. Zhang, D. Zhang, H.L. Zhu,"Ensemble of local and global information for finger-knuckle-print recognition," Pattern Recognition, To appear

[24] L. Zhang, L. Zhang, D. Zhang, H. Zhu,"Online finger-knuckle-print verification for personal authentication," Pattern Recognition, vol. 3, no. 7, pp. 2560-2571, 2010

[25] Z.H. Guo, D. Zhang, L. Zhang, W.M. Zuo," Palmprint verification using binary orientation co-occurrence vector," Pattern Recognition Letters, vol. 30, no. 13, pp. 1219-1227, 2009

[26] D. Zhang, F.X. Song, Y. Xu, Z.Z. Liang, "Advanced Pattern Recognition Technologies with Applications to Biometrics", Medical Information Science Reference, 2009